2019

Mathematical Modeling of Type 1 Diabetes

Gianna Wu
Harvey Mudd College/Pomona College

Mathematical Modeling for Type 1 Diabetes

Gianna Wu

Professor Lisette de Pillis, Advisor

Professor Blerta Shtylla, Reader

Department of Mathematics

May, 2019

Abstract

Type 1 Diabetes (T1D) is an autoimmune disease where the pancreas produces little to no insulin, which is a hormone that regulates blood glucose levels. This happens because the immune system attacks (and kills) the beta cells of the pancreas, which are responsible for insulin production. Higher levels of glucose in the blood could have very negative, long term effects such as organ damage and blindness.

To date, T1D does not have a defined cause nor cure, and research for this disease is slow and difficult due to the invasive nature of T1D experimentation. Mathematical modeling provides an alternative approach for treatment development and can greatly advance T1D research. This thesis describes both a single-compartment and multi-compartment model for Type 1 Diabetes.

Contents

List of Figures

List of Tables

Acknowledgments

I would like to thank my thesis advisor, Professor de Pillis, for guiding me through this project and for making sure that I not only succeed in all of my endeavors, but that I also take care of myself. Without you, I would not have had the amazing opportunity to work on a project that hits so close to home. I would also like to thank my second reader, Professor Shtylla, for taking the time to help me edit my thesis.

Additionally, I would like to thank my friends and family for supporting me on this project. Shout out to Davis Catolico for being my number one supporter; I am eternally grateful for your love and support. Also, shout out to Paul Mesa for not letting me give up and reminding me that I am “so close". We made it! Lastly, thanks to Tim Gaskin for getting me a shot glass to celebrate the completion of this thesis and for always being there for me through my highs and lows.

Chapter 1

Introduction

1.1 Motivation

Diabetes Mellitus, also known as Type 1 Diabetes (T1D), is a condition in which a person is unable to produce a specific hormone called insulin to regulate glucose levels in the blood, resulting in high blood glucose levels.

β-cells, which reside in the islet of Langerhans in the pancreas, are responsible for producing insulin. Insulin's main purpose is to regulate glucose in the blood by stimulating cells to absorb the glucose. For people with T1D, however, the T-cells of the immune system attack and kill off these β-cells. The cause of the autoimmune attack is currently unknown, but some potential factors could be a viral infection or environmental factors.

To date, there is no cure for T1D; the only known treatment is insulin therapy. Management of T1D requires daily injections of insulin, either through needle injections or an insulin pump. Despite this treatment, patients with Type 1 Diabetes are at a larger risk for serious health problems, such as vision loss and heart, kidney, and liver damage.

According to statistics made by the Children's Hospital in Los Angeles, about one in 500 people are affected by T1D in the United States. Additionally, the cost of healthcare for diabetes is approximately 15 billion dollars per year, and about 80 people are diagnosed with Type 1 Diabetes in the United States each day. In essence, T1D is affecting millions of people in the United States and costing billions of dollars each year.

Scientists have been researching various treatments for Type 1 Diabetes, such as dendritic cell therapy. Dendritic cells (DCs) are thought to reduce or mitigate the severity of the autoimmune attack on β-cells. More background

on the effects of dendritic cells are available in Section 1.2.

Shtylla et al. (2019) have developed a single-compartment model that incorporate β-cell populations, DC populations, macrophage populations, and T-cells populations. An overview of this model is provided in Chapter 2. The rest of this thesis uses the single-compartment model as the foundation for a newly-developed multi-compartment model. Originally, we wanted to do dynamical systems analysis on the single-compartment model. However, this model is highly nonlinear, making the analysis very complicated. Thus, we attempted to simplify the model in a way that would allow a dynamical systems analysis. However, the preliminary simplified model that we observed were not adequate in reflecting biological outcomes of real-world data. Therefore, we went in a different direction and implemented a multi-compartment model that would better reflect real-world data. The implementation of this multi-compartment model will more easily allow for the addition of a treatment compartment. The work on parameter stochasticity, sampling, and model simplification can be found in Chapter 3. The multi-compartment model can be found in Chapter 4. Chapter 5 contains the discussion and future works for this project.

1.2 Biological Background

Type 1 Diabetes occurs when the immune system loses self-tolerance to the autoantigens presented by β-cells in the pancreas (Lo et al. (2018)). This means that the immune system loses its recognition of the antigens, which are foreign substances or toxins in the body, that the β-cells present. Because of this loss in tolerance, parts of the immune system start to attack and kill the β-cells. Since β-cells are in charge of producing insulin, this results in a disruption in the production of insulin, resulting in high blood glucose levels and the eventual development of T1D.

The immune system can be categorized into two parts: an innate response and an adaptive response. The innate response cells, such as macrophages and dendritic cells (DC), continuously circulate throughout the body and consume foreign or dead cells. They also act as messengers and can evoke an adaptive immune response as necessary, as stated in Gee (2018).

Both macrophages and DCs are antigen-presenting cells (APCs), meaning that these cells mediate an adaptive immune response by processing and presenting antigens for recognition by lymphocytes like T-cells. When the immune system starts to lose tolerance of the antigens presented by β-cells, the APCs (more prominently, the DCs) present these same antigens on their surface, evoking the adaptive response. Dendritic cells themselves can be separated into two categories: tolerogenic and immunogenic. The tolerogenic DCs signal for a more neutral immune response and encourage tolerance of the foreign cells. The immunogenic DCs, on the other hand, provide a signal that evokes a more aggressive immune response attack to eliminate the targeted cells.

One of the key players of the adaptive immune response are the T-cells. In this thesis, we will focus on three types of T-cells: effector, memory, and regulatory T-cells. The effector T-cells are responsible for attacking any cell that presents the unrecognized antigen, usually signaled by the immunogenic DCs. The memory T-cells are inactive T-cells that keep track of the encountered antigens and provide a faster immune response should the pathogen be presented again. Lastly, the regulatory T-cells, which are usually summoned by tolerogenic DCs, promote tolerance to foreign cell antigens by suppressing the effects of effector T-cells.

Chapter 2

Previous Model

2.1 Derivation of Single Compartment Model

This chapter provides an overview of the previously developed single-compartment model for Type 1 Diabetes and previous simulations of the model. The following chapters will rely on the foundation work of this model.

The test subjects in the mathematical models presented in this thesis are non-obese diabetic (NOD) mice and Balb-c (healthy) mice. The dynamics of T1D have been thoroughly studied in mice but not in humans, since it is more difficult and invasive to retrieve data from human test subjects. Since there are small differences between T1D in mice versus humans, creating mathematical models for T1D in mice can inform us on the processes and bodily functions of Type 1 Diabetes in humans.

There are twelve key variables in the single compartment model for Type 1 Diabetes, separated into five categories: macrophages, β-cells, dendritic cells, the immune system's T-cells, and glucose/insulin. Their roles are further described in the following paragraphs.

Table 2.1 shows the 12 variables and their meanings. This table is slightly modified from the table in the thesis written by M. Gee. We also show the interactions of these 12 variables in Figure 2.1.

The development of T1D has been linked with lower clearance rates of macrophages in NOD mice compared to rates in Balb-c mice. Thus, the model reflects this difference by having lower macrophage clearance rates in sick mice. In this model, we represent two populations of macrophages: regular and activated. Activated macrophages differ from regular macrophages in

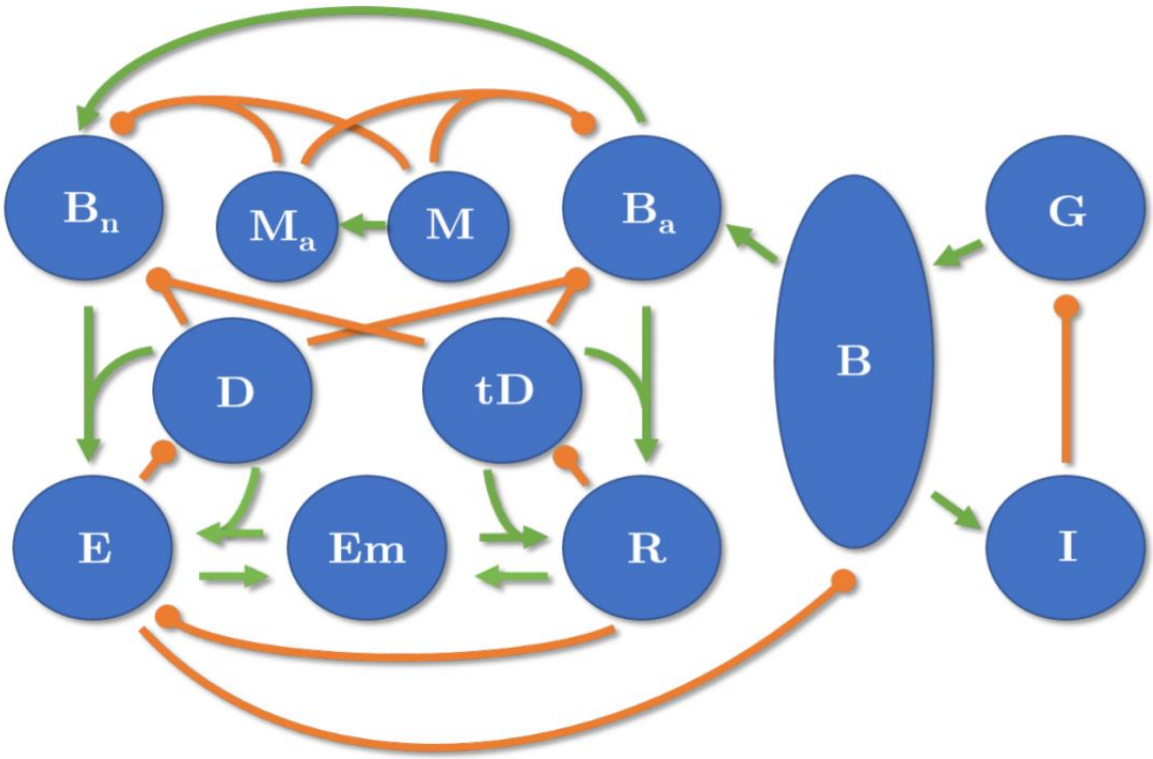

Figure 2.1 Here is the diagram of how the twelve different kind of cell populations interact with each other. The green arrows indicate that the cell population that the arrow is coming from increases or contributes to the population to which the arrow is pointing. On the other hand, the orange line segment represents that the cell population that the segment starts from inhibits or decreases the cell population to which the segment is pointing (the population where the circle end is).

Variable name	Units	Meaning	Initial Value
B	mg	Healthy β-cell population	300 mg
G	mg dl^{-1}	Glucose levels	100 mg dl^{-1}
I	μ U	Insulin levels	10 μ U
M	cells ml^{-1}	Macrophage population	$4.77 \cdot 10^5$ cells ml^{-1}
M_a	cells ml^{-1}	Active macrophage population	0 cells ml^{-1}
B_a	cells ml^{-1}	Apoptotic β-cell population	0 cells ml^{-1}
B_n	cells ml^{-1}	Necrotic β-cell population	0 cells ml^{-1}
D	cells ml^{-1}	Immunogenic DC population	0 cells ml^{-1}
tD	cells ml^{-1}	Tolerogenic DC population	0 cells ml^{-1}
E	cells ml^{-1}	Effector T-cell population	0 cells ml^{-1}
R	cells ml^{-1}	Regulatory T-cell population	0 cells ml^{-1}
Em	cells ml^{-1}	Memory T-cell population	0 cells ml^{-1}

Table 2.1 This is the complete list of variables and their initial values involved in the single-compartment model, which are originally derived in Shtylla et al. (2019).

that they have engulfed at least a necrotic or apoptotic β-cell. Because of this engulfment, the activated macrophages are able to present the autoantigens that apoptotic or necrotic β-cells produce, which notifies the immune system and potentially triggers an immune response (Maree et al. (2006)).

Additionally, a naturally occurring pre-programmed wave of cell death, known as the apoptotic wave, has also been found to contribute to the progression of T1D, as discovered in Trudeau et al. (2000). Figure 2.2 shows the previously-derived results of β-cell dynamics under four different cases: NOD mice with the apoptotic wave, NOD mice without the wave, Balb-c mice with the wave, and Balb-c mice without the wave.

This model separates β-cells into three categories: healthy β-cells, apoptotic β-cells (dying β-cells), and necrotic β-cells (dead β-cells).

We note that T-cells in the immune system are responsible for attacking and killing the healthy β-cells. Thus, in the model, this cell population is represented in three categories: effector T-cells, regulatory T-cells, and memory T-cells. We note that the effector T-cells are the main contributors for the adaptive immune response mentioned in the previous section, whereas the regulatory T-cells are responsible for building up a tolerance to foreign antigens (in this case, the β-cell autoantigens). Lastly, memory T-cells are inactive T-cells that retain their previous immune response and can quickly

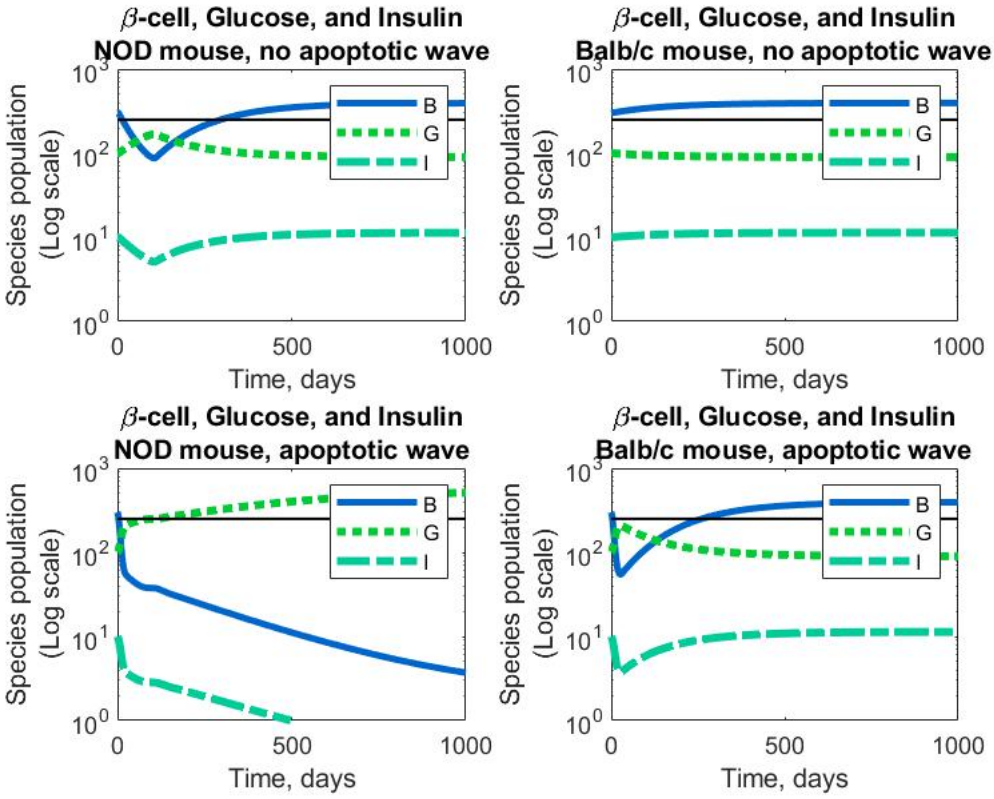

Figure 2.2 Here are the results of running the simulation on four different cases: NOD mouse without wave, Balb/c mouse without wave, NOD mouse with wave, and Balb/c mouse with wave. Only the case of NOD mouse with wave do we have the development of Type 1 Diabetes, as indicated by the increase in glucose levels, decrease in the population of β-cells, and the decrease in the amount of insulin. This figure was previously created in the paper by Shtylla et al. (2019).

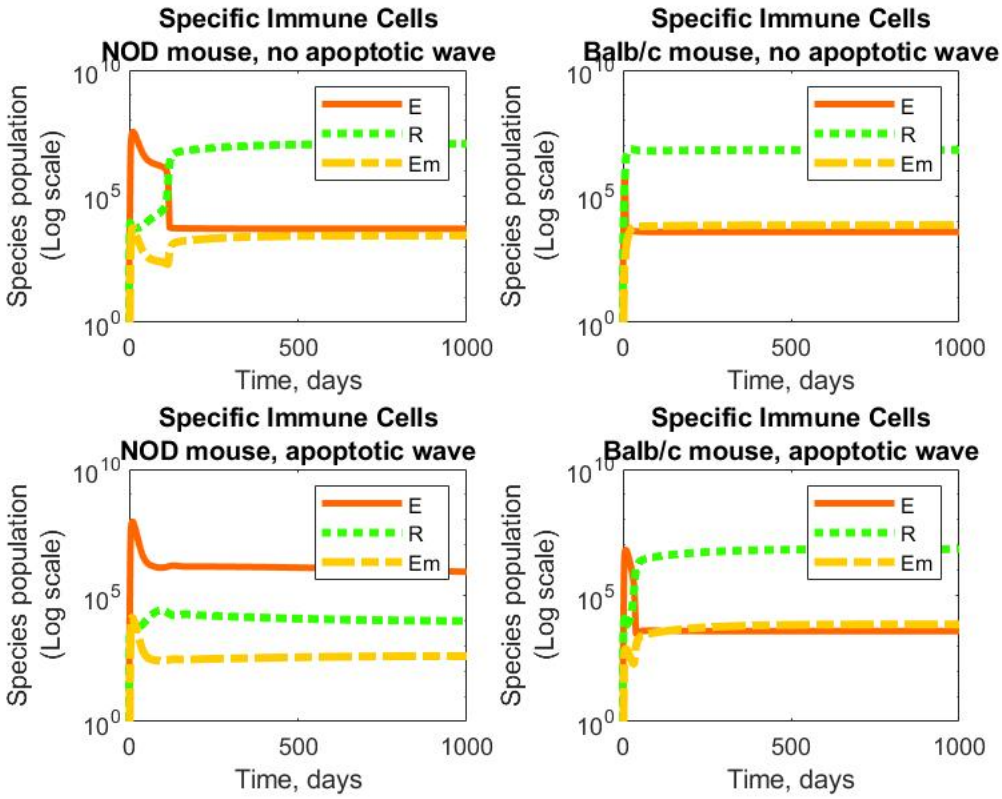

Figure 2.3 These plots show the behavior of the immune cells (E, R, and Em) in the presence/absence of a wave in both NOD and Balb-c mice.

transform back to either a regulatory or effector cell to provide a quicker immune response in the future. The previously-acquired results for the immune cell population dynamics can be seen in Figure 2.3.

We also track the populations of immunogenic and tolerogenic dendritic cells, because the DCs are responsible for triggering the adaptive immune system response. Previously-derived results of dendritic cell dynamics can be seen in Figure 2.4.

The dynamics of glucose and insulin are a crucial part of creating a mathematical model for Type 1 Diabetes, as we indicate the distinction between healthy and diabetic by an increase or spike in blood glucose levels.

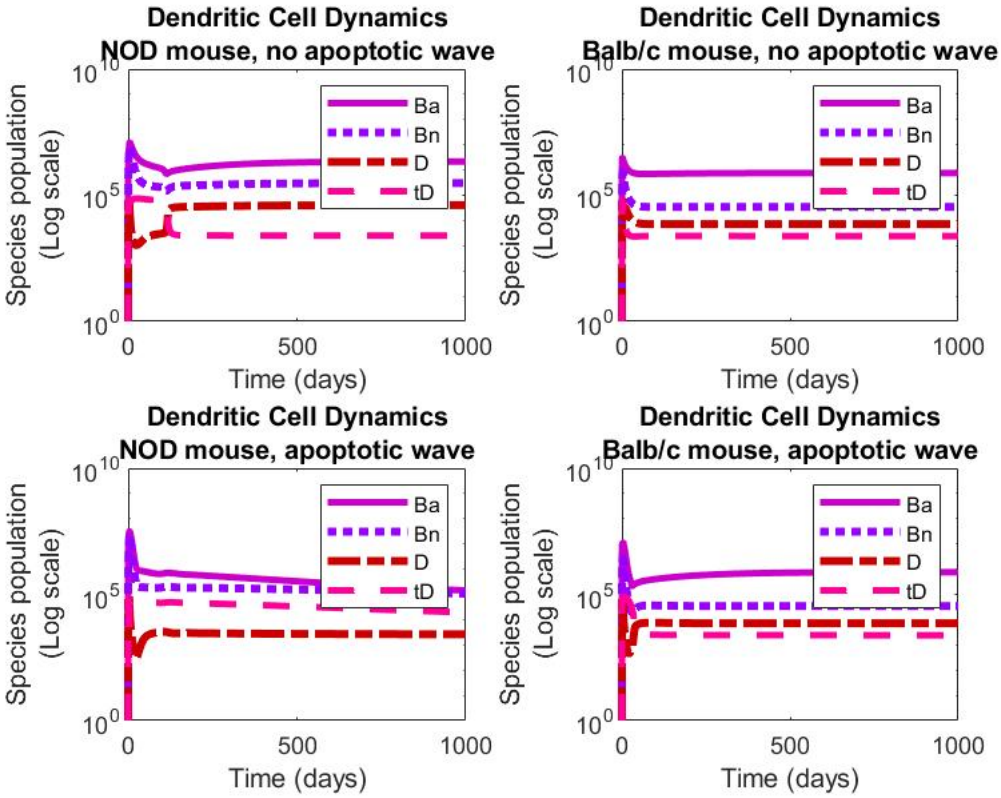

Figure 2.4 The dynamics of the dendritic cells in the single-compartment model can be seen here for all four cases.

2.2 System of Equations

This section outlines each of the 12 differential equations used to create the single-compartment model.

Macrophage Populations

$$\frac{d}{dt}M = J + (k+b)M_a - cM - f_M MB_a - f_M MB_n - e_1 M(M + M_a) \quad (2.1)$$

In this equation, we assume that macrophages are flowing in at a constant rate, J. Additionally, we assume that activated macrophages (M_a) revert back to regular macrophages (M) at a rate of k. We also know that activated macrophages recruit macrophages at a rate of b. Thus, the two interactions with M_a results in the $(k+b)M_a$ term in the equation. We also see that macrophages "leave" or "egress" at a rate of c, hence the $-cM$ term. Also note that when a macrophage consumes an apoptotic or necrotic β-cell, the macrophage transforms into an activated macrophage. The clearance rate (AKA engulfment rate) of β-cells for macrophages (M) is f_M. Thus, when necrotic or apoptotic β-cells interact with a macrophage, the population of macrophages is decreased at a rate of f_M, thus explaining the $-f_M MB_a$ and $-f_M MB_n$ terms. Lastly, the term $-e_1 M(M + M_a)$ represents the decrease in population of M due to the crowding effect.

Activated Macrophages Populations

$$\frac{d}{dt}M_a = f_M MB_a + f_M MB_n - kM_a - e_2 M_a(M + M_a) \quad (2.2)$$

Many of the terms in the M_a equation are similar to those of the M equation. As mentioned earlier, we note that macrophages become activated macrophages at a rate of f_M, which is shown by the $+f_M MB_a$ and $+f_M MB_n$ terms in the equation. Also as described before, activated macrophages revert back to macrophages at a rate of k, which is shown through the $-kM_a$ term. The last term of the equation represents the crowding effect. We note that, in Equation 2.1, the coefficient in front is e_1 whereas in Equation 2.2, the coefficient is e_2. For this model, e_1 and e_2 have the same value, since the crowding effect affects the macrophages and the activated macrophages equally.

Healthy β-cell Populations

$$\frac{d}{dt}B = \alpha_B K_1(G)B - \delta_B B - \eta K_2(E,R)B - W(B,t) \tag{2.3}$$

The first term contains $K_1(G)$, which is a function relating the population of healthy β-cells to glucose. In other words, healthy β-cells grow in proportion to the glucose levels $K_1(G)$ at a rate of α_B. In the paper, the function $K_1(G)$ is defined as:

$$K_1(G) = \frac{G^2}{G^2 + G_{hb}^2}.$$

This function was defined in Graham (2012).

The second term $-\delta_B B$ indicates that healthy β-cells are dying at a rate of δ_B.

The third term contains a function $K_2(E,R)$, which is the function that defines the interaction between T-cells and healthy β-cells. In other words, the healthy β-cells are dying in proportion to T cells at a rate of η. The function K_2, which is originally shown in Moore and Adler (2014), is defined as follows:

$$K_2(E,R) = \frac{(s_E E)^2}{1 + (s_E E)^2 + (s_R R)^2.}$$

Lastly, the fourth term represents healthy β-cell death due to the natural occurrence of an apoptotic wave, as first postulated in Trudeau et al. (2000). We define $W(B,t)$ as:

$$W(B,t) = 0.1Be^{-(\frac{t-9}{9})^2}.$$

This equation implies that the wave peaks at approximately nine days to 10 percent of the healthy β-cell population.

Apoptotic β-cell Populations

$$\frac{d}{dt}B_a = \tilde{\delta_B}B + \tilde{\eta}K_2(E,R)B + \tilde{W}(B,t) - dB_a - f_M M B_a - f_{M_a} M_a B_a \\ - f_{tD}(D_{ss} - D)B_a - f_D D B_a \tag{2.4}$$

First note that the notation for $\tilde{\delta_B}$, $\tilde{\eta}$ and $\tilde{W}$ indicates that we take the original parameters (δ_B, η, W) and multiply it by a constant, $\frac{B_{conv}}{Q_{panc}}$ for unit conversion. The original units for B is milligrams, whereas the units for B_a and B_n are cells/mL.

The first term represents the conversion of healthy β-cells to apoptotic β-cells at a rate of δ (with unit conversion). The second term represents the conversion due to normal apoptosis by T effector cells at a rate of η, again with unit conversion. The third term represents the conversion of healthy β-cells to apoptotic cells due to the pre-programmed wave of cell death. Included also is a death rate d for B_a. We also note that macrophages and activated macrophages are able to clear away the apoptotic β-cells at rates of f_M and f_{M_a}, respectively. In addition, dendritic cells are able to engulf or clear away necrotic cells. All immature DCs, represented as $D_{ss} - D$ in the equation, can clear apoptotic β-cells at a rate of f_{tD}, whereas mature/immunogenic DCs, represented by D, can clear at a rate of f_D.

Necrotic β-cell Populations

$$\frac{d}{dt}B_n = dB_a - f_M M B_n - f_{M_a} M_a B_n - f_{tD}(D_{ss} - D)B_n - f_D D B_n \tag{2.5}$$

We note that B_a are converted to necrotic β-cells at a death rate of d. Very similarly to the apoptotic β-cell population, macrophages, activated macrophages, immature (tolerogenic) dendritic cells, and immunogenic dendritic cells are able to clear necrotic β-cells at rates of f_M, f_{M_a}, f_{tD}, and f_D respectively.

Glucose

$$\frac{d}{dt}G = R_0 - (G_0 + S_I I)G \tag{2.6}$$

For this equation, we assume that glucose enters the bloodstream at a constant rate of R_0. We also assume that glucose leaves the bloodstream at a constant rate of G_0. Additionally, glucose is decreased in the presence of insulin at a rate of S_I. This equation and the equation for insulin were originally derived in Topp et al. (2000).

Insulin

$$\frac{d}{dt}I = \sigma_I \frac{G^2}{G^2 + GI^2} B - \delta_I I \tag{2.7}$$

Insulin is produced at a rate (σ_I) proportional to the population of healthy β-cells in the presence of glucose. Lastly, insulin has a natural decay rate of δ_I.

Immunogenic Dendritic Cell Populations

$$\frac{d}{dt}D = f_{tD}B_n(D_{ss} - D - tD) + f_{tD}B_n tD - b_{DE}ED - \mu_D D \tag{2.8}$$

D_{ss} represents a constant steady state of naive dendritic cells in the pancreas. When these naive DCs, represented by $(D_{ss} - D - tD)$, engulf necrotic β-cells at a rate of f_{tD}, they become immunogenic DCs. Tolerogenic DCs can become activated immunogenic DCs upon engulfing a necrotic cell at a rate of f_{tD}. Immunogenic DCs are removed by effector T-cells (E) at a rate of b_{DE} and have a death rate of μ_D.

Tolerogenic Dendritic Cell Populations

$$\frac{d}{dt}tD = f_{tD}B_a(D_{ss} - D - tD) - f_{tD}B_n tD - b_{IR}RtD - \mu_D tD. \tag{2.9}$$

When the naive DCs (represented by $D_{ss} - D - tD$) engulf apoptotic β-cells at a rate f_{tD}, they become tolerogenic DCs. As mentioned before, tolerogenic DCs convert to immunogenic DCs upon engulfing a necrotic β-cell at a rate of f_{tD}, thus explaining the $-f_{tD}B_n tD$ term. Regulatory T-cells remove tolerogenic DCs at a rate of b_{IR}. Also, tolerogenic DCs have a death rate of μ_D, similar to the equation for immunogenic DCs derived in Ludewig et al. (2004).

Effector T-cell Populations

$$\frac{d}{dt}E = a_E\left(\frac{T_{naive}}{Q_{spleen}} - E\right) + b_P\frac{DE}{\theta_D + D} - r_{am}E + b_E DEm - \mu_E ER \tag{2.10}$$

The first term in this equation represents a homeostatic naive T-cell term that generates effector T-cells. The second term represents the immunogenic DC-induced proliferation of effector T-cells. This happens at the same rate b_P for both E and R. We note that θ_D is the DC value for half-maximal effector T-cell expansion. The $r_{am}E$ term represents the reversion of effector cells to memory cells at a rate of r_{am}. We note that effector T-cells are reactivated (from memory T-cells) by immunogenic DCs at a rate of b_E, as shown by the $b_E DE_m$ term. Lastly, regulatory T-cells supress the actions ("shut down" the inflammatory response) of the effector T-cells at a rate of μ_E. Another way to interpret μ_E is that this is the rate at which effector T-cells are removed due to competition between effector and regulatory T-cells, as stated in Ludewig et al. (2004).

Regulatory T-cell Populations

$$\frac{d}{dt}R = a_R\left(\frac{T_{naive}}{Q_{spleen}} - R\right) + b_P\frac{tDR}{\theta_D + tD} - r_{am}R + b_R tDEm - \mu_R ER \quad (2.11)$$

The regulatory T-cell equation is very similar to the effector T-cell equation. The first term still represents a homeostatic naive T-cell population that generates regulatory T-cells at a rate of α_R. We note that α_R is equal to α_E from the previous equation in this model. Additionally, the second term represents the tD-induced proliferation of regulatory T-cells at a rate of b_P. Regulatory T-cells convert to memory T-cells at a rate of r_{am} and are reactivated by tolerogenic DCs at a rate of b_R. The last term in this equation serves the same purpose as the last term of the previous equation. We note that in our model, $\mu_R = \mu_E$.

Memory T-cell Populations

$$\frac{d}{dt}Em = r_{am}(E + R) - (a_{Em} + b_E D + b_R tD)Em \quad (2.12)$$

As mentioned above, both effector and regulatory T-cells are reverted to memory T-cells at a rate of r_{am}. We also mentioned that dendritic cells reactive the T-cells with rates of b_E and b_R, which leads to a decrease in the population of E_m. Lastly, memory T-cells have a death rate of a_{E_m}.

2.3 Parameter Values

Table 2.2 shows the values of the parameters used in the single-compartment model. Many of these parameters will also be used in the multi-compartment model, which is described in Chapter 4.

Parameter	Balb-c mice	NOD mice	Units	Meaning
J	$5 \cdot 10^4$	$5 \cdot 10^4$	cells ml^{-1} d^{-1}	normal resting macrophage influx
k	0.4	0.4	d^{-1}	Ma deactivation rate
b	0.09	0.09	d^{-1}	macrophage recruitment rate by M_a
c	0.1	0.1	d^{-1}	macrophage egress rate
f_M	$2 \cdot 0.0623 \cdot 10^{-5}$	$0.0623 \cdot 10^{-5}$	ml cell^{-1} d^{-1}	basal phagocytosis rate per M for Balb-c mice
e_1	10^{-8}	10^{-8}	cell^{-1} d^{-1}	anti-crowding term for macrophages
e_2	10^{-8}	10^{-8}	cell^{-1} d^{-1}	anti-crowding term for macrophages
α_B	0.0334	0.0334	d^{-1}	β-cell growth rate
δ_B	1/60	1/60	d^{-1}	β-cell death rate
η	0.02	0.02	d^{-1}	rate at which T-cells eliminate β-cells
G_{hb}	90	90	mg dl^{-1}	glucose level of half-max β-cell production
s_E	1	1	ml cells^{-1}	Relative impact of effector T-cells on β-cell death
s_R	36	36	ml cells^{-1}	Relative impact of regulatory T-cells on β-cell death
B_{conv}	$2.59 \cdot 10^5$	$2.59 \cdot 10^5$	cell mg^{-1}	β-cells per milligram
Q_{panc}	0.194	0.194	ml	volume of mouse pancreas
d	0.50	0.50	d^{-1}	β-cell death rate
f_{Ma}	$5 \cdot 0.0623 \cdot 10^{-5}$	$0.0623 \cdot 10^{-5}$	ml cells^{-1} d^{-1}	activated phagocytosis rate per Ma
f_{tD}	$1.1899 \cdot 10^{-6}$	$1.1899 \cdot 10^{-6}$	ml cells^{-1} d^{-1}	rate naive DC engulf apoptotic β-cells
D_{ss}	10^5	10^5	cells ml^{-1}	steady-state DC population

f_D	$1.7101 \cdot 10^{-7}$	$1.7101 \cdot 10^{-7}$	ml cells^{-1} d^{-1}	rate naive DC engulf necrotic β-cells
R_0	864	864	mg dl^{-1}	basal rate glucose production
G_0	1.44	1.44	d^{-1}	rate of glucose decay
S_I	0.72	0.72	ml μU^{-1} d^{-1}	insulin rate of glucose elimination
σ_I	43.2	43.2	μU ml^{-1} d^{-1} mg^{-1}	maximum rate of insulin production by β-cells
GI	141.4214	141.4214	mg dl^{-1}	glucose level of half-max insulin production
δ_I	432	432	d^{-1}	rate of insulin decay
b_{DE}	$0.487 \cdot 10^{-5}$	$0.487 \cdot 10^{-5}$	ml cells^{-1} d^{-1}	DC elimination rate by effector T-cells
μ_D	0.51	0.51	d^{-1}	DC death rate
b_{IR}	$0.487 \cdot 10^{-5}$	$0.487 \cdot 10^{-5}$	ml cells^{-1} d^{-1}	DC elimination rate by regulatory T-cells
a_E	0.1199	0.1199	d^{-1}	rate of initial expansion of naive T-cells to effector T-cells
T_{naive}	370	370	cells	number of naive T-cells contributing to initial production of effector and regulatory T-cells
Q_{spleen}	0.1	0.1	ml	volume of mouse spleen
b_p	12	12	d^{-1}	maximum expansion rate of effector T-cells due to DCs
θ_D	$2.12 \cdot 10^5$	$2.12 \cdot 10^5$	d^{-1}	DC value for half-maximal effector T-cell expansion
r_{am}	0.01	0.01	d^{-1}	reversion rate of T-cells to memory T-cells

b_E	10^{-3}	10^{-3}	ml d cells^{-1}	activation rate for effector T-cells from memory T-cells
μ_E	$2 \cdot 10^{-6}$	$2 \cdot 10^{-6}$	d^{-1}	effector T-cell removal rate due to competition
a_R	0.1199	0.1199	d^{-1}	rate of initial expansion of naive T-cells to regulatory T-cells
b_R	10^{-3}	10^{-3}	ml d cells^{-1}	activation rate for regulatory T-cells from Em T-cells
μ_R	$2 \cdot 10^{-6}$	$2 \cdot 10^{-6}$	d^{-1}	regulatory T-cell removal rate due to competition
a_{Em}	0.01	0.01	d^{-1}	memory T-cell death rate

Table 2.2 A list of the parameters used in the single-compartment model. This list was derived from the original paper by Shtylla et al. (2019).

2.4 Remaining Open Questions of the Model

Something worth noting is that, when including a DC treatment in the model, there seemed to be a window of opportunity for which dosages of treatment would work and otherwise wouldn't work. The previously-obtained results can be seen in Figure 2.5.

One explanation of this has to do with the ratio of regulatory T-cells to effector T-cells. Regulatory T-cells mitigate the inflammatory response that the effector T-cells have, thus building up a tolerance to the unknown antigen presented in the body. The higher the ratio, the smaller the immune response. Ideally, we want the immune response to be reduced so that healthy β-cells are not accidentally killed off by the effector T-cells. In Figure 2.6, the graph of R/E seems very similar to the graph of the dosage levels. This is a strong indicator of why the window of opportunity for dosaging exists.

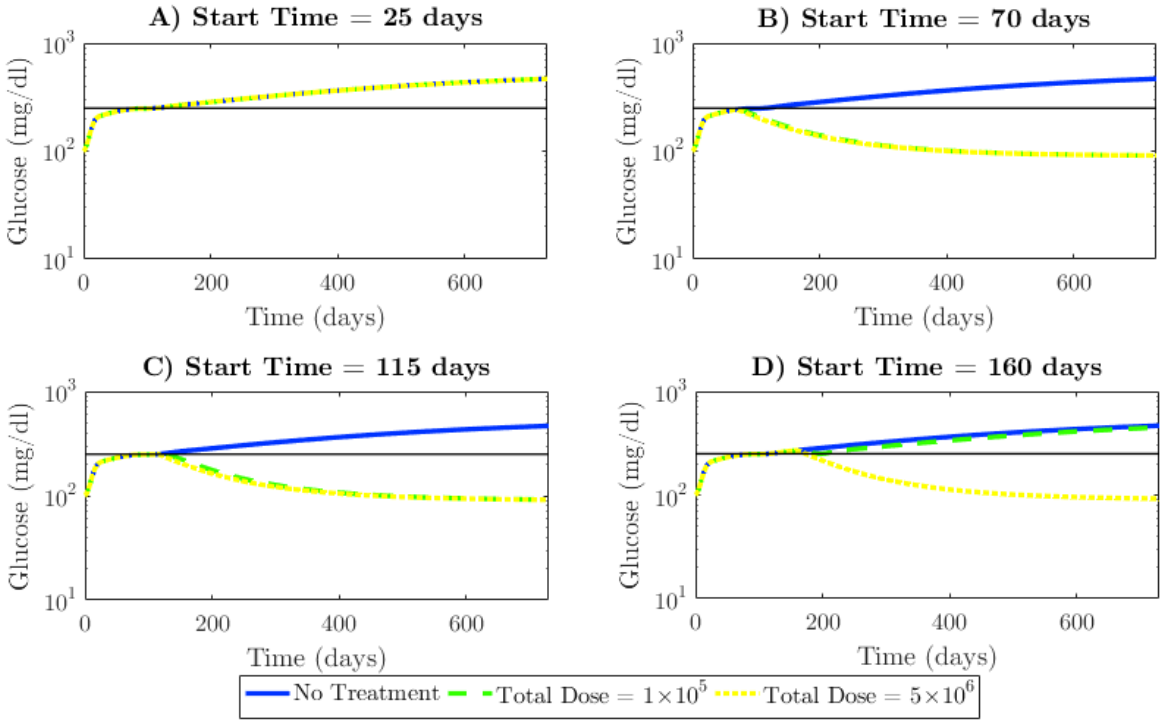

Figure 2.5 This figure shows the effects of various levels of treatment dosage on glucose levels. If the treatment is injected too early, it is ineffectual (panel A). If the treatment is injected between (roughly) 70 and 160 days, then both low and high levels of dosage will work. However, after 160 days, the low dosage no longer works. This indicates that there exists an optimal time frame in which to inject treatment to prevent the onset of T1D. This figure was created in Shtylla et al. (2019).

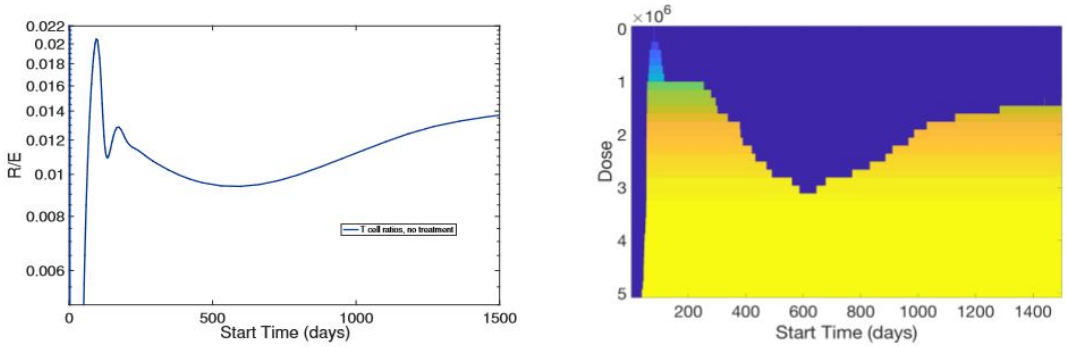

Figure 10. The NOD mouse model simulated with a dose of tolerogenic DCs administered at a series of treatment start times. The ratio of T regulatory vs T effector cells is measured at the end of each 2000 day simulation for multiple single doses administered at various treatment start days. We illustrate regions of effectiveness that qualitatively agree with simulation results for doses in the low treatment range $(0.5 - 1.5e5)$, intermediate doses $2 - 2.3e5$ and high doses $3e5 - 5e6$.

Figure 2.6 The shape of the graph for the ratio of regulatory T-cells to effector T-cells and the graph for dosage levels are very similar. This ratio may be the cause for the “window of opportunity". This figure is from Shtylla et al. (2019).

Chapter 3

Supplementary Work on the Single-Compartment Model

3.1 Model Simplification

One of the earliest goals of this thesis was to perform dynamical systems analysis. However, dynamical systems analysis would be very difficult (if not impossible) since the current single-compartment model is highly nonlinear. Thus, before performing any sort of analysis, we wanted to see if we could simplify the model. Specifically, we wanted to linearize the glucose and insulin equations. In Makroglou et al. (2006), they had a minimal model for glucose and insulin. The model that was developed in Makroglou et al. (2006) is as follows:

$$\frac{dG(t)}{dt} = -[b_1 + X(t)]G(t) + b_1 G_b,$$

$$\frac{dX(t)}{dt} = -b_2 X(t) + b_3[I(t) - I_b],$$

$$\frac{dI(t)}{dt} = b_4[G(t) - b_5]^+ t - b_6[I(t) - I_b],$$

where G is glucose, X is "an auxiliary function representing insulin-excitable tissue glucose uptake activity", and I is insulin. Unfortunately, this equation did not fit well with the single-compartment model. Thus, instead of continuing to pursue model simplification, we instead went in a different direction with the model.

3.2 Stochasticity

The next goal after an attempt at model simplification was to incorporate stochasticity into the model. From Li et al. (2010), we were able to see blood glucose levels in various untreated NOD mice. We wanted to be able to incorporate stochasticity into the model so that we could replicate the results in figure 3.1.

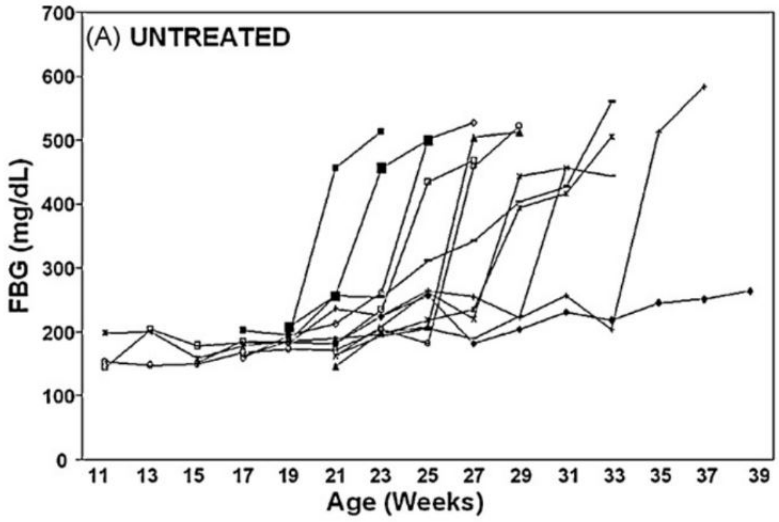

Figure 3.1 The blood glucose levels were tracked in untreated NOD mice.

In Figure 3.1, we see various possibilities for the onset of Type 1 Diabetes. There could be an early onset, delayed onset, fast onset, and slow onset. We wanted to be able to represent all four kinds of onset in our model. Thus, we experimented with randomly choosing parameter values within a healthy range. In the beginning, we chose the two most sensitive variables to experiment with: f_M, which is the clearance rate of macrophages, and μ_R, which is the removal rate for regulatory T-cells due to competition. Results of this can be found in Figure 3.2.

3.3 Parameter Sampling

Because some combinations of f_M and μ_R could drive the simulation to a healthy state, we wanted to experiment with other parameters relating to

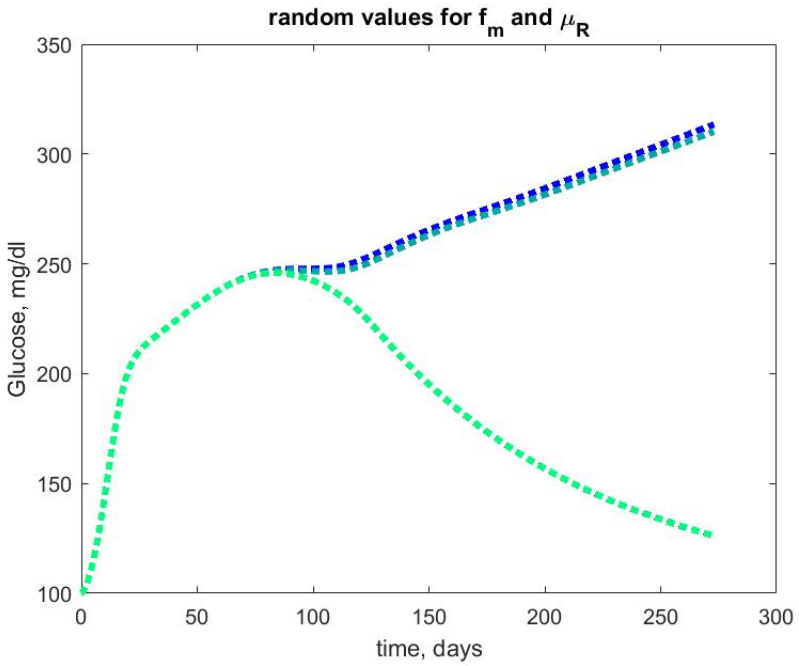

Figure 3.2 This is a graph of the blood glucose levels vs. time when the f_M and μ_R parameters have randomized values within a reasonable range. With some combinations of f_M and μ_R values, the simulation goes towards a healthy state, whereas with other combinations, it tends towards a diabetic state instead.

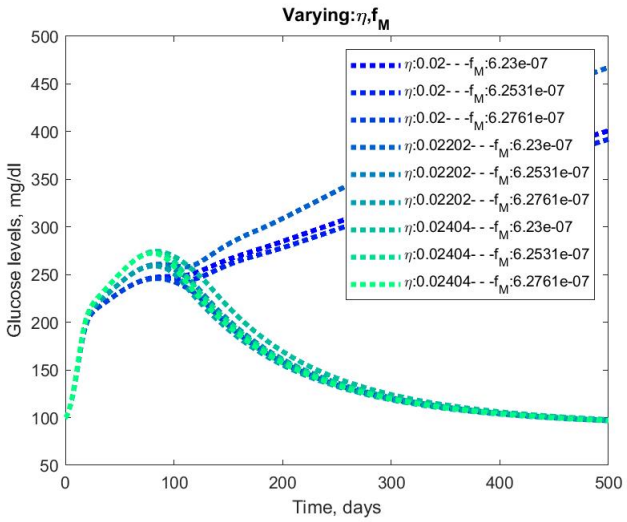

Figure 3.3 Varying η and f_M.

the innate immune system to see if we could get the various types of onset. Thus, the next step was to take all of the parameters relating to the immune system and vary them against each other in pairs. The table of parameters that we varied can be found in Table 3.1.

For the parameters with a sensitivity value of ±50%, this meant that during the parameter sensitivity testing, their sensitivities were higher than 50%. Thus, we arbitrarily varied their values by ±50%.

With the single-compartment model, we were able to get the fast spiking, early spiking, and slow spiking when varying two parameters at a time. However, we were unable to get the delayed spiking. Figures 3.3, 3.4, and 3.5 show some examples of the combinations that we get.

Unfortunately, we still did not see the delayed spiking that was seen in the real-world data. Thus, we turned to creating a multi-compartment model for Type 1 Diabetes with the hopes of better reflecting the real-world data. The multi-compartment model is covered in depth in the next chapter.

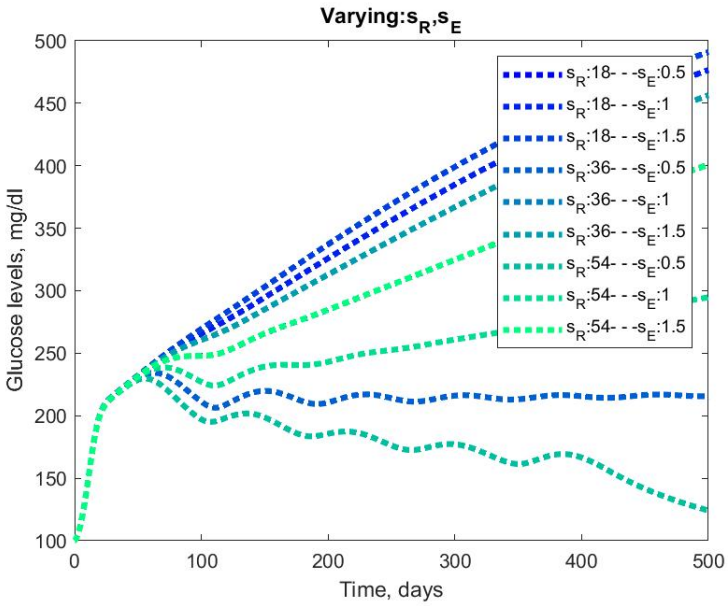

Figure 3.4 Varying s_R and s_E against each other.

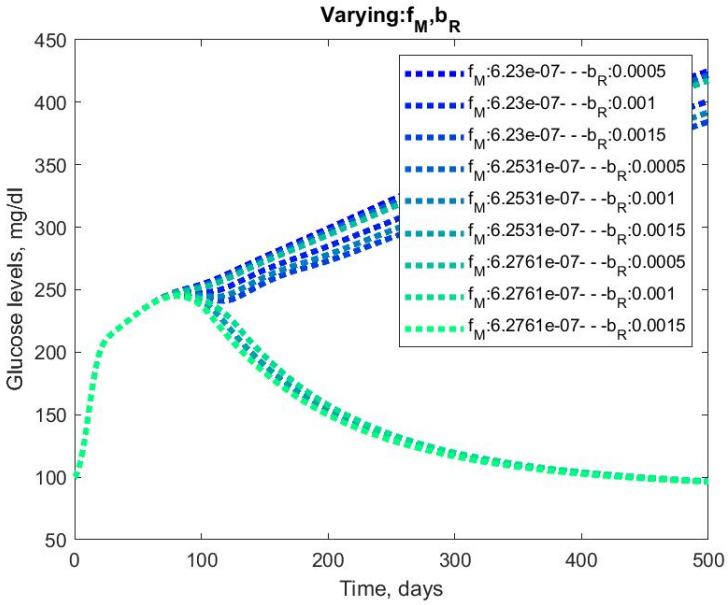

Figure 3.5 Varying f_M and b_R.

parameter	meaning	value	sensitivity
η	rate at which T-cells eliminate β-cells	0.02 days^{-1}	+20.2%
s_R	relative impact of R on β-cell death	36 ml cells^{-1}	± 50%
s_E	relative impact of E on β-cell death	1 ml cells^{-1}	± 50%
f_{M_a}	rate M_a engulf B_n and B_a	0.0623×10^{-5} ml cells^{-1} days^{-1}	+1.7%
f_M	rate M engulf B_n and B_a	0.0623×10^{-5} ml cells^{-1} days^{-1}	+0.74%
f_{tD}	rate naive DCs engulf B_a	1.19×10^{-6} ml cells^{-1} days^{-1}	-1.3%
f_D	rate naive DCs engulf B_n	1.71×10^{-7} ml cells^{-1} days^{-1}	±50%
μ_R	rate of R removal due to competition	5×10^{-6} d^{-1}	−0.684%
b_R	R activation rate from E_m	1×10^{-3} ml d cells^{-1}	±50%
μ_E	rate of E removal due to competition	5×10^{-6} d^{-1}	+2.8%
b_E	E activation rate from E_m	1×10^{-3} ml d cells^{-1}	−45.2%
b_P	maximal expansion rate of E due to DCs	12 d^{-1}	−23.5%
a_R	rate of initial expression of naive T-cells into R	0.1199 d^{-1}	+1.2%
a_E	rate of initial expression of naive T-cells into E	0.1199 d^{-1}	+1.2%
b_{IR}	rate of elimination of tDCs by R	0.487×10^{-5} ml cells^{-1} d^{-1}	−12.3%
b_{DE}	rate of elimination of DCs by E	0.487×10^{-5} ml cells^{-1} d^{-1}	±50%
b	M recruitment rate by M_a	0.09 d^{-1}	−0.92%

Table 3.1 Table of sampled parameters and their sensitivity values, derived from Gee (2018).

Chapter 4

Multi-Compartment Model

4.1 Introduction

As mentioned previously, we want to be able to replicate the real world data with our mathematical model. With the single-compartment model, we were able to get early spiking, slow spiking, and fast spiking. However, we were unable to get the delayed spiking. Thus, we wanted to transform the single-compartment model into a multi-compartment model. A lot of the groundwork for this model was done by Professors de Pillis and Shtylla. However, for this thesis, adjustments were made, and the macrophage and activated macrophage populations were incorporated.

The multi-compartment model consists of three separate compartments: the bloodstream, the spleen, and the pancreas. Figure 4.1 shows the model diagram.

The full diagram can be seen in Figure 4.2. Similar to the diagram in Figure 2.1 for the single-compartment model, this diagram shows how the cells in each compartment interact with each other and with cells from other compartments.

4.2 Variables

We outline the 23 different variables used in this model in Table 4.1, along with their initial conditions.

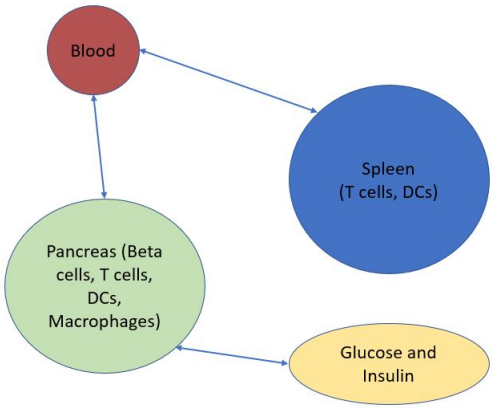

Figure 4.1 This is a diagram of the different kinds of compartments in our multi-compartment model.

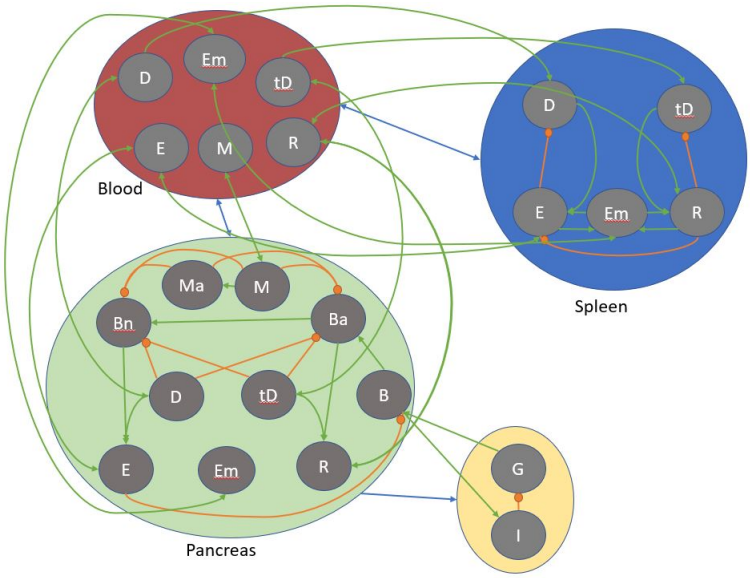

Figure 4.2 Here is the full model diagram showing the interactions between all of the cells.

Variable name	Units	Meaning	Initial Value
B	mg	Healthy β-cell population	300 mg
G	mg dl^{-1}	Glucose levels	100 mg dl^{-1}
I	μU	Insulin levels	10 μU
M	cells ml^{-1}	Macrophage population in the pancreas	0 cells ml^{-1}
M_b	cells ml^{-1}	Macrophage population in the blood	$4.77 \cdot 10^5$ cells ml^{-1}
M_a	cells ml^{-1}	Activated macrophage population in the pancreas	0 cells ml^{-1}
B_a	cells ml^{-1}	Apoptotic β-cell population	0 cells ml^{-1}
B_n	cells ml^{-1}	Necrotic β-cell population	0 cells ml^{-1}
D_{panc}	cells ml^{-1}	Immunogenic DC population in the pancreas	0 cells ml^{-1}
D_s	cells ml^{-1}	Immunogenic DC population in the spleen	0 cells ml^{-1}
D_{blood}	cells ml^{-1}	Immunogenic DC population in the blood	0 cells ml^{-1}
tD_{panc}	cells ml^{-1}	Tolerogenic DC population in the pancreas	0 cells ml^{-1}
tD_s	cells ml^{-1}	Tolerogenic DC population in the spleen	0 cells ml^{-1}
tD_{blood}	cells ml^{-1}	Tolerogenic DC population in the blood	0 cells ml^{-1}
E_{panc}	cells ml^{-1}	Effector T-cells in the pancreas	0 cells ml^{-1}
E_s	cells ml^{-1}	Effector T-cells in the spleen	0 cells ml^{-1}

E_{blood}	cells ml^{-1}	Effector T-cells in the blood	0 cells ml^{-1}
R_{panc}	cells ml^{-1}	Regulatory T-cells in the pancreas	0 cells ml^{-1}
R_s	cells ml^{-1}	Regulatory T-cells in the spleen	0 cells ml^{-1}
R_{blood}	cells ml^{-1}	Regulatory T-cells in the blood	0 cells ml^{-1}
Em_{panc}	cells ml^{-1}	Memory T-cells in the pancreas	0 cells ml^{-1}
Em_s	cells ml^{-1}	Memory T-cells in the spleen	0 cells ml^{-1}
Em_b	cells ml^{-1}	Memory T-cells in the blood	0 cells ml^{-1}

Table 4.1 A list of the 23 variables used in the multi-compartment model with their initial conditions.

4.3 Equations

We have three separate compartments: the spleen, the pancreas, and the blood. The blood compartment is mostly used from transporting cells from one compartment to the other.

Spleen Compartment

DCs in the Spleen

$$\frac{d}{dt}D_s = \left(\frac{Q_{blood}}{Q_{spleen}}\right)\mu_B D_b - a_D D_s - b_{DE} D_s E_s \tag{4.1}$$

This equation represents the behavior of the immunogenic dendritic cells in the spleen. We note that any μ term will typically represent an emigration rate unless otherwise stated. In this case, dendritic cells from the bloodstream (D_b) are coming into the spleen at a rate of μ_B. We also have a conversion rate $\left(\frac{Q_{blood}}{Q_{spleen}}\right)$ because the volumes of the blood and spleen compartment are different, and concentration is the usual unit of measure for this model. Dendritic cells in the spleen are also dying at a rate of a_D. Lastly, the $b_{DE} D_s E_s$ term represents the same phenomenon as in the single-compartment model:

dendritic cells in the spleen are being eliminated by effector T-cells in the spleen (E_s) at a rate of b_{DE}.

$$\frac{d}{dt}tD_s = \left(\frac{Q_{blood}}{Q_{spleen}}\right)\mu_B tD_b - a_I tD_s - b_{IR}tD_s R_s \tag{4.2}$$

This equation represents the behavior of the tolerogenic DCs in the spleen. Similar to the immunogenic DC equation, tolerogenic DCs in the spleen (tD_b) are emigrating at a rate of μ_B. The same conversion factor from above applies here as well. The tolerogenic DCs are also dying at a rate of a_I. Lastly, tD_b cells are eliminated by regulatory T-cells in the spleen (T_s) at a rate of b_{IR}.

T-cells in the Spleen

$$\frac{d}{dt}E_s = \left(\frac{Q_{blood}}{Q_{spleen}}\right)\mu_{BSE}E_b - \mu_{SB}(D_s)E_s + b_E D_s E m_s + a_E\left(\frac{T_{naive}}{Q_{spleen}} - E_s\right) - \mu_E E_s R_s - r_{am}E_s + b_p\frac{D_s E_s}{\theta_D + D_s} \tag{4.3}$$

This equation represents the behavior of effector T-cells. Effector T-cells are exiting the blood and entering the spleen at a rate of μ_{BSE}. We note that because of the difference in compartment volumes, we have to do a conversion, indicated by $\left(\frac{Q_{blood}}{Q_{spleen}}\right)$. We also note that $\mu_{SB}(D_s)$ is a gating term represented by:

$$\mu_{SB}(DC) = \mu^*_{SB} + \frac{\Delta_\mu}{1 + \frac{DC}{\theta_{shut}}} \tag{4.4}$$

where $\Delta_\mu = \mu^{normal}_{SB} - \mu^*_{SB}$. This term represents the dendritic cells signaling the activated CTLs (cytotoxic T lymphocytes) to flow from the spleen to the blood. The flow of these T-cells is restricted, as modeled by the gating term. Similar to the single-compartment model, memory T-cells are being reactivated as effector T-cells by immunogenic DCs at a rate of b_E, effector T-cells are being generated at a rate of a_E, effector T-cells are being removed due to competition with the regulatory T-cells at a rate of μ_E, effector T-cells are reverting back to memory T-cells at a rate of r_{am}, and effector T-cells are proliferating due to DCs, which is represented by the $b_P\frac{D_s E_s}{\theta_D + D_s}$ term.

$$\frac{d}{dt}R_s = \left(\frac{Q_{blood}}{Q_{spleen}}\right)\mu_{BSE}R_b - \mu_{SB}(tD_s)R_s + b_R tD_s Em_s + a_R\left(\frac{T_{naive}}{Q_{spleen}} - R_s\right) - \mu_R E_s R_s - r_{am}R_s + b_P\frac{tD_s R_s}{\theta_D + tD_s} \quad (4.5)$$

This equation represents the behavior of the regulatory T-cells in the spleen. We note that this equation is very similar to the effector T-cells equation - the slight differences are that tolerogenic DCs (tD_s) interact with the regulatory T-cells (R) instead of immunogenic DCs (D_s) with effector T-cells (E), and the parameters are labeled differently. b_R is the rate at which memory T-cells are being converted to tolerogenic DCs, and a_R is the rate at which R is being generated from naive T-cells.

$$\frac{d}{dt}Em_s = \left(\frac{Q_{blood}}{Q_{spleen}}\right)\mu_{BSE}Em_b - \mu_{SB}(D_s)Em_s + r_{am}(E_s + R_s) - (a_{Em} + b_E D_s + b_R tD_s)Em_s \quad (4.6)$$

This equation represents the behavior of memory T-cells in the spleen. We note that the first two terms are very similar to the E_s and R_s equations. The $r_{am}(E_s + R_s)$ term represents effector and regulatory T-cells converting to memory T-cells at a rate of r_{am}. a_{Em} is the death rate, and memory T-cells are converted back to effector and regulatory T-cells by immunogenic DCs and tolerogenic DCs at rates of b_E and b_R, respectively.

Blood Compartment

DCs in the Bloodstream

$$\frac{d}{dt}D_b = -\mu_B D_b + \left(\frac{Q_{panc}}{Q_{blood}}\right)\mu_{PB}D_{panc} \quad (4.7)$$

This is the equation for immunogenic dendritic cells in the blood. We note that μ_B is the rate at which DCs are leaving the blood (to enter the spleen compartment). μ_{PB} represents the DC emigration rate from the pancreas to the blood. Again, we have a conversion factor to account for the difference in compartment volumes.

$$\frac{d}{dt}tD_b = -\mu_B tD_b + \left(\frac{Q_{panc}}{Q_{blood}}\right)\mu_{PB}tD_{panc} \quad (4.8)$$

This is the equation for tolerogenic DCs in the blood. We note that this equation is almost identical to the immunogenic DCs equation - the only change is that D_b is replaced with tD_b to represent tolerogenic DC behavior in the blood.

T-cells in the Bloodstream

$$\frac{d}{dt}E_b = \left(\frac{Q_{spleen}}{Q_{blood}}\right)\mu_{SB}(D_s)E_s + \left(\frac{Q_{panc}}{Q_{blood}}\right)\mu_{PB}E_{panc} - (\mu_{BP} + \mu_{BSE})E_b \quad (4.9)$$

$$\frac{d}{dt}R_b = \left(\frac{Q_{spleen}}{Q_{blood}}\right)\mu_{SB}(tD_s)R_s + \left(\frac{Q_{panc}}{Q_{blood}}\right)\mu_{PB}R_{panc} - (\mu_{BP} + \mu_{BSE})R_b \quad (4.10)$$

$$\frac{d}{dt}Em_b = \left(\frac{Q_{spleen}}{Q_{blood}}\right)\mu_{SB}(D_s)Em_s + \left(\frac{Q_{panc}}{Q_{blood}}\right)\mu_{PB}Em_{panc} - (\mu_{BP} + \mu_{BSE})Em_b \quad (4.11)$$

The above equations are for the effector T-cells, regulatory T-cells, and memory T-cells in the blood, respectively. Recall that $\mu_{SB}(D_s)$ represents the gating term mentioned previously. We also have the conversion rate $\left(\frac{Q_{spleen}}{Q_{blood}}\right)$ in order to properly measure concentration, since the blood has a different volume than the spleen. μ_{PB} represents the emigration rate from the pancreas to the blood. We have the conversion rate $\left(\frac{Q_{panc}}{Q_{blood}}\right)$ to account for the difference in volume for the pancreas and the blood. For the last term, we have that the T-cells are flowing out of the blood stream and into the pancreas and spleen compartment at a rate of μ_{BP} and μ_{BSE} respectively.

Macrophages in the Bloodstream

$$\frac{d}{dt}M_b = -J_{new} + \left(\frac{Q_{panc}}{Q_{blood}}\right)c_{new}M \quad (4.12)$$

This equation is a new addition to the multi-compartment model, since the fundamental multi-compartment model did not include macrophages. We assume that the macrophages start in the bloodstream and enter the tissue (pancreas) at a constant rate J_{new}. J_{new} is related to J, the original macrophage influx rate in the single-compartment model, through the following equation: $J_{new}\left(\frac{Q_{blood}}{Q_{panc}}\right) = J$. Something to note here is that J in the single-compartment model has the value of $5 \cdot 10^4$ cells ml^{-1} d^{-1}, which was taken from Maree

et al. (2006). However, this is a rounded value, and Maree et al. (2006) cites the more correct estimation to be approximately $4.8 \cdot 10^4$ cells ml^{-1} d^{-1}. Thus, we use this closer approximation for our J value.

We also assume that macrophages leave the pancreas and enter the bloodstream at a rate of c_{new}. This parameter is the same parameter c used in the single-compartment model. However, we note that the value of c can be ranged from 0.07 to 0.25, as stated in Maree et al. (2006). So, in the multi-compartment model, $c_{new} = 0.117$.

Pancreas Compartment

β-cells in the Pancreas

Below is the equation for the healthy β-cell populations. This equation is identical to the equation in the single-compartment model.

$$\frac{d}{dt}B = \alpha_B K_1(G)B - \delta_B B - W(B,t) - \eta K_2(E_{panc}, R_{panc})B \tag{4.13}$$

where

$$K1(G) = \frac{G^2}{G^2 + G_{hb}^2}$$

is the function relating the population of healthy β-cells to glucose.

$$K2(E_{panc}, R_{panc}) = \frac{(s_E E_{panc})^2}{1 + (s_E E_{panc})^2 + (s_R R_{panc})^2}$$

is the function that defines the interaction between T-cells and healthy β-cells.

$$W(B,t) = 0.1Be^{-(\frac{t-9}{9})^2}$$

is the function representing the apoptotic wave.

Below is the equation for the apoptotic β-cells. This equation is also identical to the equation presented in the single-compartment model.

$$\begin{aligned}\frac{d}{dt}B_a = \tilde{W}(B,t) + \tilde{\eta}K2(E_{panc}, R_{panc})B - f_M M B_a - f_{Ma} M_a B_a \\ - dB_a + \tilde{\delta_B} B - f_{tD}(D_{ss} - D_{panc})B_a - f_D D_{panc} B_a\end{aligned} \tag{4.14}$$

Lastly, this equation represents the necrotic β-cells.

$$\frac{d}{dt}B_n = dB_a - f_M M B_n - f_{M_a} M_a B_n - f_{tD}(D_{ss} - D_{panc})B_n - f_D D_{panc} B_n \tag{4.15}$$

The equations for the healthy, apoptotic, and necrotic β-cells in this multi-compartment model are identical to those presented in the single-compartment model, because we assume that β-cells stay and interact with other cells solely in the pancreas.

DCs in the Pancreas

$$\frac{d}{dt}D_{panc} = f_{tD}B_n(D_{ss} - D_{panc} - tD_{panc}) + f_{tD}B_n tD_{panc} - \mu_{PB}D_{panc} \quad (4.16)$$

$$\frac{d}{dt}tD_{panc} = f_{tD}B_a(D_{ss} - D_{panc} - tD_{panc}) - f_{tD}B_n tD_{panc} - \mu_{PB}tD_{panc}. \quad (4.17)$$

The equations for immunogenic and tolerogenic DCs in the pancreas are similar. For the immunogenic DCs, naive dendritic cells are converted into immunogenic DCs at a rate of f_{tD} when encountering a necrotic β-cell. Likewise, when a naive dendritic cell encounters an apoptotic β-cell, it transforms into a tolerogenic DC. Lastly, both immunogenic and tolerogenic DCs emigrate out of the pancreas into the bloodstream at a rate of μ_{PB}.

T-cells in the Pancreas

$$\frac{d}{dt}E_{panc} = \left(\frac{Q_{blood}}{Q_{panc}}\right)\mu_{BP}E_b - \mu_{PB}E_{panc} \quad (4.18)$$

$$\frac{d}{dt}R_{panc} = \left(\frac{Q_{blood}}{Q_{panc}}\right)\mu_{BP}R_b - \mu_{PB}R_{panc} \quad (4.19)$$

$$\frac{d}{dt}Em_{panc} = \left(\frac{Q_{blood}}{Q_{panc}}\right)\mu_{BP}Em_b - \mu_{PB}Em_{panc} \quad (4.20)$$

The three equations above all have the same structure. T-cells are coming into the pancreas at a rate μ_{BP}. Because the pancreas and the blood have different volume sizes, we require a conversion term, $\left(\frac{Q_{blood}}{Q_{panc}}\right)$. Lastly, T-cells are leaving the pancreas to the blood at a rate of μ_{PB}.

Macrophages in the Pancreas

$$\frac{d}{dt}M = \left(\frac{Q_{blood}}{Q_{panc}}\right)J_{new} + (k+b)Ma - c_{new}M - f_M MBa - f_M MB_n - e_1 M(M+Ma) \quad (4.21)$$

This equation is almost identical to the equation for macrophages in the single-compartment model. The only differences are the $J_{new}\left(\frac{Q_{blood}}{Q_{panc}}\right)$ term to represent the influx of macrophages to the pancreas and the c_{new} to denote the macrophage egress rate to the blood. We note that since the macrophages are flowing in from the blood compartment, we must convert the J_{new} term so that it uses the appropriate volume term. However, $J_{new}\left(\frac{Q_{blood}}{Q_{panc}}\right) = J$, where J is the parameter used in the original single-compartment model.

$$\frac{d}{dt}Ma = f_M MBa + f_M MB_n - kMa - e_2 Ma(M + Ma) \tag{4.22}$$

This equation is exactly the same as the equation presented in the single-compartment model for activated macrophages.

Glucose and Insulin

$$\frac{d}{dt}G = R_0 - (G_0 + S_I I)G \tag{4.23}$$

$$\frac{d}{dt}I = \sigma_I \frac{G^2}{G^2 + GI^2}B - \delta_I I \tag{4.24}$$

We remark that the glucose and insulin equations in the multi-compartment model are identical to the equations found in the single-compartment model.

4.4 Parameter Values

Many of the parameters shown in Table 2.2 for the single-compartment model are used in the multi-compartment model. However, the multi-compartment model also requires new parameters (such as migration rates from/to compartments). Thus, all parameters used in the multi-compartment model are listed in Table 4.1.

Parameter	Balb-c mice	NOD mice	Units	Meaning
μ_B	74.56	74.56	day^{-1}	dendritic cell emigration rate from blood to spleen
Q_{blood}	3	3	ml	volume of mouse blood compartment

a_D	0.2310	0.2310	day^{-1}	death rate of immunogenic DCs in the spleen
a_I	0.2310	0.2310	day^{-1}	death rate of tolerogenic DCs in the spleen
μ_{BSE}	0.0220	0.0220	day^{-1}	T-cell emigration rate from blood to spleen
μ_{PB}	0.51	0.51	day^{-1}	emigration rate of DCs and T-cells from the pancreas to the blood
μ_{BP}	0.1	0.1	day^{-1}	emigration rate of DCs and T-cells from the blood to the pancreas
J_{new}	$3.2333 \cdot 10^3$	$3.2333 \cdot 10^3$	cells ml^{-1} d^{-1}	normal resting macrophage influx
μ^*_{SB}	0.012	0.012	day^{-1}	CTL migration rate from the spleen to blood at equilibrium
μ^{normal}_{SB}	0.1120	0.1120	day^{-1}	normal CTL migration rate from spleen to blood
Δ_μ	0.1	0.1	day^{-1}	$\mu^{normal}_{SB} - \mu^*_{SB}$
c_{new}	0.117	0.117	day^{-1}	macrophage egress rate
k	0.4	0.4	d^{-1}	Ma deactivation rate
b	0.09	0.09	d^{-1}	macrophage recruitment rate by M_a
f_M	$2 \cdot 0.0623 \cdot 10^{-5}$	$0.0623 \cdot 10^{-5}$	ml cell^{-1} d^{-1}	basal phagocytosis rate per M for Balb-c mice
e_1	10^{-8}	10^{-8}	cell^{-1} d^{-1}	anti-crowding term for macrophages
e_2	10^{-8}	10^{-8}	cell^{-1} d^{-1}	anti-crowding term for macrophages
α_B	0.0334	0.0334	d^{-1}	β-cell growth rate
δ_B	1/60	1/60	d^{-1}	β-cell death rate
η	0.02	0.02	d^{-1}	rate at which T-cells eliminate β-cells

G_{hb}	90	90	mg d^{-1}	glucose level of half-max β-cell production
s_E	1	1	ml $cells^{-1}$	Relative impact of effector T-cells on β-cell death
s_R	36	36	ml $cells^{-1}$	Relative impact of regulatory T-cells on β-cell death
B_{conv}	$2.59 \cdot 10^5$	$2.59 \cdot 10^5$	cell mg^{-1}	β-cells per milligram
Q_{panc}	0.194	0.194	ml	volume of mouse pancreas
d	0.50	0.50	d^{-1}	β-cell death rate
f_{Ma}	$5 \cdot 0.0623 \cdot 10^{-5}$	$0.0623 \cdot 10^{-5}$	ml $cells^{-1}$ d^{-1}	activated phagocytosis rate per Ma
f_{tD}	$1.1899 \cdot 10^{-6}$	$1.1899 \cdot 10^{-6}$	ml $cells^{-1}$ d^{-1}	rate naive DC engulf apoptotic β-cells
D_{ss}	10^5	10^5	cells ml^{-1}	steady-state DC population
f_D	$1.7101 \cdot 10^{-7}$	$1.7101 \cdot 10^{-7}$	ml $cells^{-1}$ d^{-1}	rate naive DC engulf necrotic β-cells
R_0	864	864	mg dl^{-1}	basal rate glucose production
G_0	1.44	1.44	d^{-1}	rate of glucose decay
S_I	0.72	0.72	ml μU^{-1} d^{-1}	insulin rate of glucose elimination
σ_I	43.2	43.2	μU ml^{-1} d^{-1} mg^{-1}	maximum rate of insulin production by β-cells
GI	141.4214	141.4214	mg dl^{-1}	glucose level of half-max insulin production
δ_I	432	432	d^{-1}	rate of insulin decay
b_{DE}	$0.487 \cdot 10^{-5}$	$0.487 \cdot 10^{-5}$	ml $cells^{-1}$ d^{-1}	DC elimination rate by effector T-cells
μ_D	0.51	0.51	d^{-1}	DC death rate

b_{IR}	$0.487 \cdot 10^{-5}$	$0.487 \cdot 10^{-5}$	ml cells^{-1} d^{-1}	DC elimination rate by regulatory T-cells
a_E	0.1199	0.1199	d^{-1}	rate of initial expansion of naive T-cells to effector T-cells
T_{naive}	370	370	cells	number of naive T-cells contributing to initial production of effector and regulatory T-cells
Q_{spleen}	0.1	0.1	ml	volume of mouse spleen
b_p	12	12	d^{-1}	maximum expansion rate of effector T-cells due to DCs
θ_D	$2.12 \cdot 10^5$	$2.12 \cdot 10^5$	d^{-1}	DC value for half-maximal effector T-cell expansion
r_{am}	0.01	0.01	d^{-1}	reversion rate of T-cells to memory T-cells
b_E	10^{-3}	10^{-3}	ml d cells^{-1}	activation rate for effector T-cells from memory T-cells
μ_E	$2 \cdot 10^{-6}$	$2 \cdot 10^{-6}$	d^{-1}	effector T-cell removal rate due to competition
a_R	0.1199	0.1199	d^{-1}	rate of initial expansion of naive T-cells to regulatory T-cells
b_R	10^{-3}	10^{-3}	ml d cells^{-1}	activation rate for regulatory T-cells from Em T-cells
μ_R	$2 \cdot 10^{-6}$	$2 \cdot 10^{-6}$	d^{-1}	regulatory T-cell removal rate due to competition
a_{Em}	0.01	0.01	d^{-1}	memory T-cell death rate

Table 4.2 Here is the list of all parameters used in the multi-compartment model. Parameters highlighted in blue are new parameters that are used exclusively in the multi-compartment model. Parameters highlighted in red (specifically, J_{new} and c_{new}) are parameters that exist in the single-compartment model but have different values. Parameters in black are parameters that have the same value in both the single-compartment and the multi-compartment model.

4.5 Results

For the NOD mice, we were able to attain diverging behaviors for NOD mice with the apoptotic wave and NOD mice without the wave. Specifically, we saw that for NOD mice experiencing the wave, there was a spike in blood glucose levels, leaving them in a diabetic state (of above 250 mg/dl).

For Balb-c mice, we see that regardless of the presence of a wave, the Balb-c mice would stay healthy, which is what we observed in the single compartment model. The results of the multi-compartment model can be seen in Figure 4.3. A comparison between the single compartment and multi-compartment model is shown in Figure 4.4.

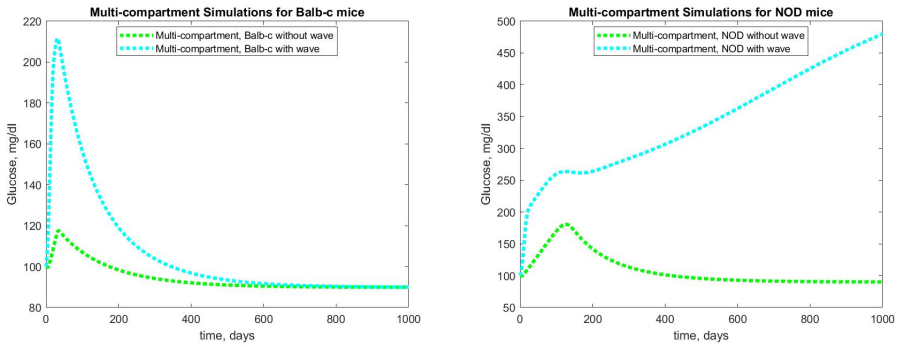

Figure 4.3 The image on the left is the result of running the multi-compartment model for Balb-c mice. The presence of the wave does not affect the glucose levels of the Balb-c mice at equilibrium. However, the result on the right shows that NOD mice will become diabetic if they experience an apoptotic wave but will stay healthy otherwise.

In Figure 2.2, we plotted the glucose, insulin, and β-cell populations for the single-compartment model. We were able to achieve similar results for the glucose, insulin, and β-cells populations for the multi-compartment

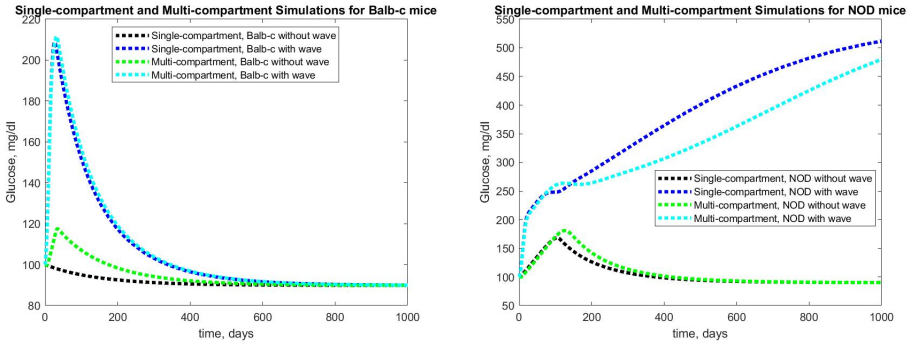

Figure 4.4 We have the results for both the single and multi-compartment models for Balb-c mice on the left. On the right is the result for both models for NOD mice. We can see that the behavior is relatively similar.

model, which can be seen in Figure 4.5.

We were also able to plot the immune cell populations in Figure 4.6 and the dendritic cell dynamics in Figure 4.7. We can compare these results to the results acquired in the single-compartment models, which are Figures 2.3 and 2.4.

4.6 Summary

We were able to create a 23-equation multi-compartment model for Type 1 Diabetes in mice. The results achieved with this model are similar to those achieved with the single-compartment model.

Specifically, we were able to take the equations for each variable in the single compartment model and separate certain interactions into their appropriate compartments. In other words, in the single-compartment model, we assumed that all variables interacted with each other in one compartment, but in the multi-compartment model, we moved some of these interactions to different compartments. For example, in the multi-compartment model, we assumed that the elimination of DCs by T-cells occurred in the spleen and thus moved that part of the DC equation (such as the $b_{IR} \cdot tD_s R_s$ term in the tolerogenic DC equation) to the spleen compartment.

While the results are similar, we still do see some minor differences between the two models. For example, in the case of the Balb-c mice that do not experience the apoptotic wave, we see a small spike in glucose levels,

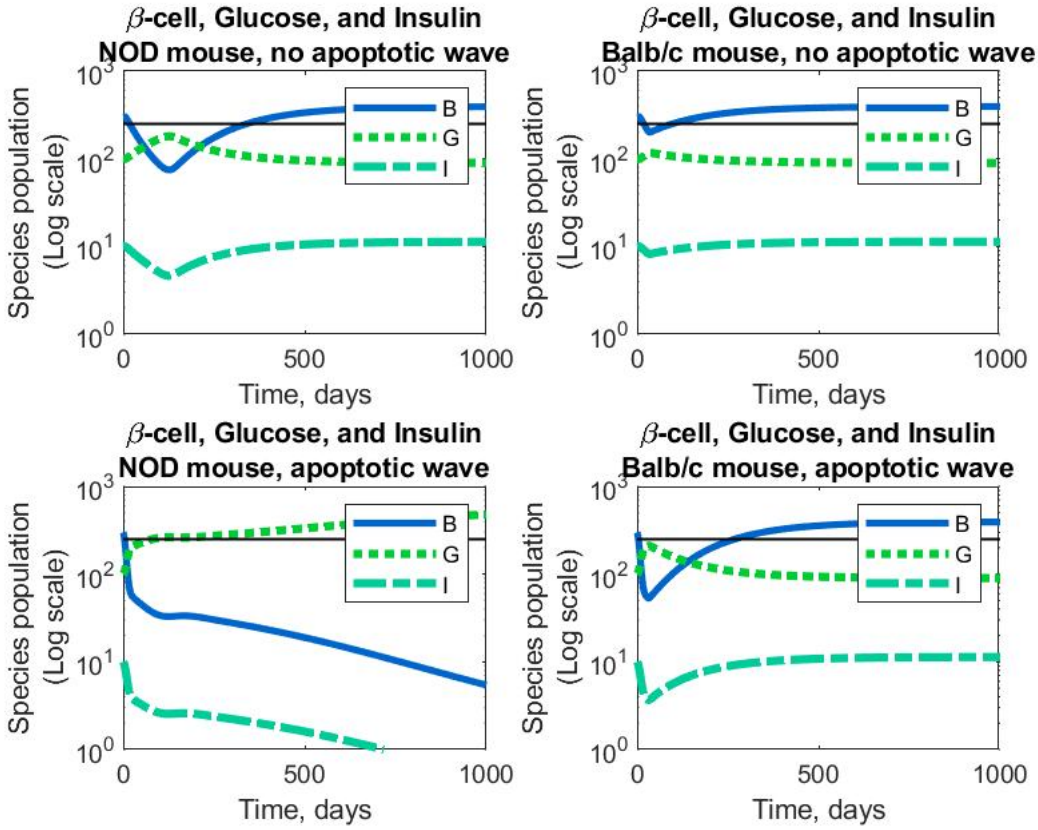

Figure 4.5 These plots show the behavior of the β-cell, glucose, and insulin populations in four different scenarios.

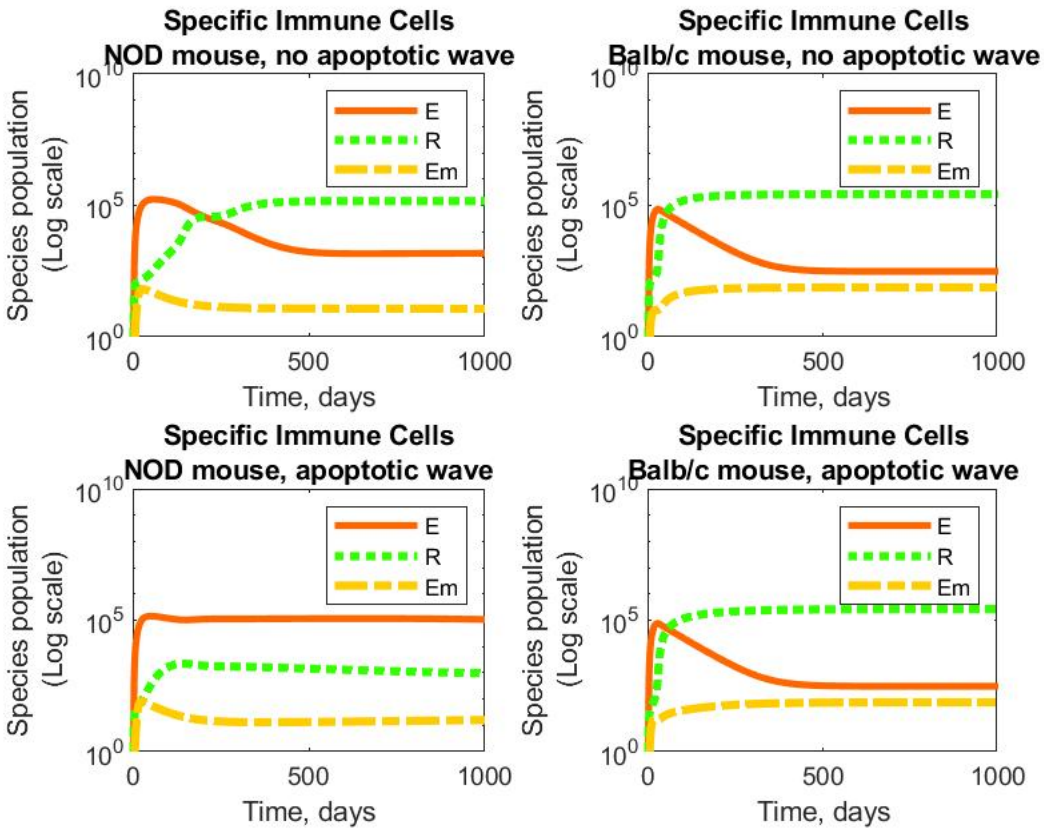

Figure 4.6 Here are the population levels for each of the three immune cells (effector, regulatory, and memory) over time. This graph is very similar to the graph obtained with the single-compartment model.

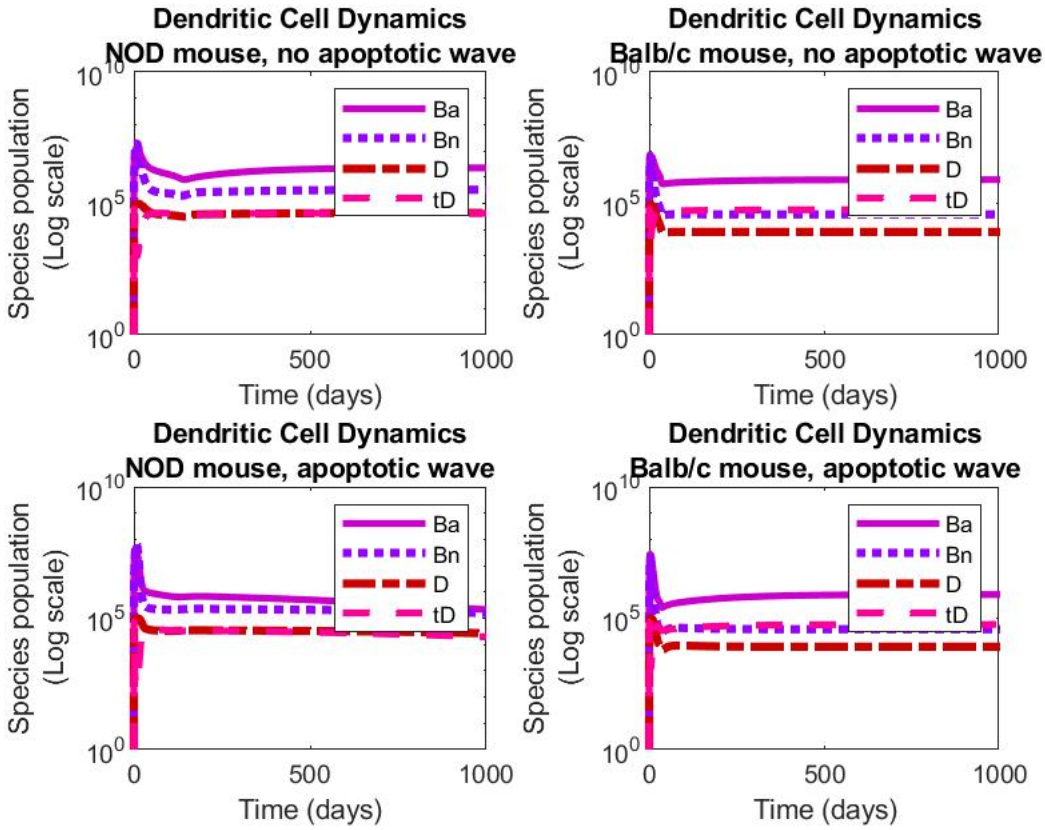

Figure 4.7 Here are the plots of the dendritic cells and β-cell populations. This behavior also matches the behavior observed in the single-compartment model.

but we do not see this spike in the single-compartment model. Further investigation is needed to determine why this spike happens and whether we can reduce or eliminate it. We also note that the behaviors of the immune cells and the DCs in the multi-compartment slightly vary from those of the single-compartment model.

The macrophages equations may also still need tweaking, since those equations are brand new and were not a part of the original multi-compartment model developed by Professors Lisette de Pillis and Blerta Shtylla. Otherwise, we may continue to work with this multi-compartment model and add a treatment compartment as well.

Chapter 5

Discussion

5.1 Conclusion

The single-compartment model for Type 1 Diabetes is a simple yet powerful tool to learn more about diabetes and allow for realistic simulations. With just a single-compartment, it is able to accurately capture data recorded in Balb-c and NOD mice. Additionally, it was able to find a window of opportunity for which treatment would be most effective. The reason behind this window of opportunity may have to do with the ratio between regulatory and effector T-cells. Lastly, we were able to add stochastic elements to the model to more accurately represent real-world data, since not all NOD mice behave in the same way. While we were able to achieve some variance, we would still like to see a delayed spike in glucose levels.

The multi-compartment is able to achieve similar results to the single-compartment. It could also be more biologically accurate, since it slightly incorporates time delays. The multi-compartment model currently includes three compartments: the blood, the spleen, and the pancreas. With the development of this model, we hope to develop a treatment compartment that will be able to more accurately capture how treatments interact with the body biologically. Currently, in the single-compartment model, we simulate treatments and injections by simply increasing both populations of dendritic cells. With the multi-compartment model, we hope to more realistically model how treatments are actually administered.

5.2 Future Work

The main goal moving forward will be to develop a biologically-accurate treatment compartment for the multi-compartment model. Additionally, we would like to perform a dynamical systems analysis on this model to analyze the stability of its fixed points.

Similar to our goals with the single-compartment model, we could try to incorporate a delay in spiking of the glucose levels. Recall that, with the real-world NOD mice data, we saw four different kinds of spiking: early, delayed, fast, and slow. We could try to model the different kinds of spiking in our multi-compartment model as well. We could also try to incorporate actual time delays in our multi-compartment model.

Another future direction would be to use this model as a foundation for modeling Type 1 Diabetes in humans. This would require research on parameter values for humans and analyzing the differences in biological dynamics between humans and mice with T1D.

Bibliography

Gee, Marissa. 2018. Modeling Type 1 Diabetes and Immune Cell Dynamics in the Pancreas .

Graham, Erica. 2012. Mathematical Models of Mechanisms Underlying Long-term Type 2 Diabetes Progression .

Jayaraman, Sundararajan, Akshay Patel, Arathi Jayaraman, Vasu Patel, Mark Holterman, and Bellur Prabhakar. 2013. Transcriptome Analysis of Epigenetically Modulated Genome Indicates Signature Genes in Manifestation of Type 1 Diabetes and Its Prevention in NOD Mice. *PLoS ONE* 8(1):e55,074. doi:10.1371/journal.pone.0055074. URL https://dx.doi.org/10.1371/journal.pone.0055074.

Khadra, Anmar, Pere Santamaria, and Leah Edelstein-Keshet. 2009. The role of low avidity T cells in the protection against type 1 diabetes: A modeling investigation. *Journal of Theoretical Biology* 256(1):126–141. doi:10.1016/j.jtbi.2008.09.019. URL http://linkinghub.elsevier.com/retrieve/pii/S0022519308004918.

———. 2010. The pathogenicity of self-antigen decreases at high levels of autoantigenicity: a computational approach. *International Immunology* 22(7):571–582. doi:10.1093/intimm/dxq041. URL https://academic.oup.com/intimm/article-lookup/doi/10.1093/intimm/dxq041.

Li, Alice, Jianfeng Chen, Masahiro Hattori, Edson Franco, Craig Zuppan, Okechukwu Ojogho, Yuichi Iwaki, and Alan Escher. 2010. A therapeutic DNA vaccination strategy for autoimmunity and transplantation. *Vaccine* 28(8):1897–1904. doi:10.1016/j.vaccine.2009.10.090. URL http://linkinghub.elsevier.com/retrieve/pii/S0264410X09016399.

Lo, Jeannette, Chang-Qing Xia, Ruihua Peng, and Michael J. Clare-Salzler. 2018. Immature Dendritic Cell Therapy Confers Durable Immune Mod-

ulation in an Antigen-Dependent and Antigen-Independent Manner in Nonobese Diabetic Mice. *Journal of Immunology Research* 2018:1–13. doi:10.1155/2018/5463879. URL https://www.hindawi.com/journals/jir/2018/5463879/.

Ludewig, Burkhard, Philippe Krebs, Tobias Junt, Helen Metters, NevilleâĂĎJ. Ford, RoyâĂĎM. Anderson, and Gennady Bocharov. 2004. Determining control parameters for dendritic cell-cytotoxic T lymphocyte interaction. *European Journal of Immunology* 34(9):2407–2418. doi:10.1002/eji.200425085. URL http://doi.wiley.com/10.1002/eji.200425085.

Mahaffy, Joseph M., and Leah EdelsteinâĂŘKeshet. 2007. Modeling Cyclic Waves of Circulating T Cells in Autoimmune Diabetes. *SIAM Journal on Applied Mathematics* 67(4):915–937. doi:10.1137/060661144. URL http://epubs.siam.org/doi/10.1137/060661144.

Makroglou, Athena, Jiaxu Li, and Yang Kuang. 2006. Mathematical models and software tools for the glucose-insulin regulatory system and diabetes: an overview. *Applied Numerical Mathematics* 56(3-4):559–573. doi:10.1016/j.apnum.2005.04.023. URL http://linkinghub.elsevier.com/retrieve/pii/S0168927405000929.

Maree, A. F.M, R. Kublik, D. T Finegood, and L. Edelstein-Keshet. 2006. Modelling the onset of Type 1 diabetes: can impaired macrophage phagocytosis make the difference between health and disease? *Philosophical Transactions of the Royal Society A: Mathematical, Physical and Engineering Sciences* 364(1842):1267–1282. doi:10.1098/rsta.2006.1769. URL http://rsta.royalsocietypublishing.org/cgi/doi/10.1098/rsta.2006.1769.

Moore, James R., and Fred Adler. 2014. Mathematical modeling of type 1 diabetes in the NOD mouse: separating incidence and age of onset. *arXiv:14126566 [q-bio]* URL http://arxiv.org/abs/1412.6566. ArXiv: 1412.6566.

Shtylla, Blerta, Marissa Gee, Shahrokh Shabahang, Leif Eldevik, and Lisette de Pillis. 2019. A mathematical model for DC vaccine treatment of type I diabetes. *Frontiers* .

Topp, Brian, Keith Promislow, Gerda Devries, Robert M Miura, and Diane T Finegood. 2000. A Model of Îš -Cell Mass, Insulin, and Glucose Kinetics: Pathways to Diabetes. *Journal of Theoretical Biology* 206(4):605–619. doi:10.1006/jtbi.2000.2150. URL http://linkinghub.elsevier.com/retrieve/pii/S0022519300921507.

Trudeau, Jacqueline D, Jan P Dutz, Edith Arany, David J Hill, Warren E Fieldus, and Diane T Finegood. 2000. A Trigger for Autoimmune Diabetes? 49:7.